THE DYNAMICS OF MUSHY LAYERS

M.G. WORSTER
Department of Engineering Sciences & Applied Mathematics
and Department of Chemical Engineering
Northwestern University
Evanston, IL 60208 USA

ABSTRACT. The development of mathematical models describing mushy zones is reviewed. Particular attention is paid to the transport of mass, heat and species in these reacting, two-phase media. Dynamical interactions between solidification in mushy regions and three different types of convection are analyzed: convection due to shrinkage or expansion upon change of phase; and buoyancy driven convection driven either by thermal gradients or by solutal gradients. Directions for future reseach into the dynamics of mushy regions are suggested.

1. Introduction

Regions of intimately coexisting liquid and solid phases, called "mushy regions" are ubiquitous during the solidification of multi-component systems. They can be viewed as the consequence of morphological instabilities of would-be, planar solid–liquid phase boundaries (Mullins & Sekerka, 1964), and serve to reduce or eliminate regions of constitutional supercooling in the system (Worster, 1986; Fowler, 1987) that arise due to the slow diffusion of chemical species relative to heat. The micro-scale morphology of mushy layers varies considerably with the chemical system being solidified (figure 1) but all are characterized by the length scale of internal phase boundaries being very much smaller than the macroscopic dimensions of the layer. This is a key feature upon which mathematical models of mushy regions are based.

It is of great importance to understand the interactions between solidification and flow of the melt, since fluid flow transports heat, which influences the rate of solidification, and transports solute, which causes segregation of the constituents of the melt. A wide range of striking fluid-mechanical effects during solidification are discussed and beautifully illustrated in a review article by Huppert (1990). Here we shall focus specifically on interactions between fluid flow and mushy regions and consider the effects of flow caused by three different physical mechanisms: the flow of interdendritic melt due to the expansion or shrinkage that occurs as one phase changes to another; thermal convection in the region of melt exterior to the mushy layer driven by undercooling at the mush–liqiud interface; and compositional convection driven by the rejection of one component of the alloy during solidification. In each case, we shall see that the flow is an inevitable consequence of

S. H. Davis et al. (eds.), Interactive Dynamics of Convection and Solidification, 113–138.

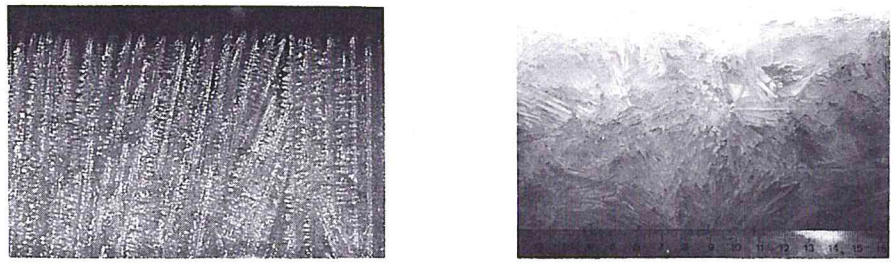

Figure 1. (a) Side view of the dendrites in a mushy layer of ammonium-chloride crystals. (b) End-on view of ice platelets in a mushy layer grown from an aqueous solution. Although different chemical systems have quite different micro-scale morphologies, the crystals in each case are much smaller than the overall dimensions of the mushy layer.

the process of solidification and examine the effect of the flow on macrosegregation of the alloy. Compositional buoyancy typically dominates thermal buoyancy in multi-component systems, though either can be the primary cause of convection depending on the geometry of the mould and the position of its cooled boundaries. On Earth, gravitational convection, whether compositionally or thermally driven, has much larger effects on a casting than does the convection due to solidification shrinkage. However, in a micro-gravitational environment, solidification shrinkage can play the dominant rôle.

Two examples of experimental castings are shown in figure 2. In each case, one of the horizontal boundaries of the mould is cooled to below the eutectic temperature, and a composite solid layer forms, separated from the melt by a mushy layer. The style of convection is quite different in the two cases, and results in the final castings having different textures and compositional variations. It is these sorts of variations that theoretical models aim to explain.

2. Mathematical Modelling of Mushy Regions

Theoretical and numerical models of mushy regions typically seek to provide descriptions of the evolving two-phase media on the macro scale, much larger than the mean spacing between solid particles. Seemingly different models of mushy regions have been formulated independently by metallurgists, engineers and applied mathematicians. On closer examination, one appreciates that the differences are related more to language and terminology than to physical content. For many years, metallurgists have made use of the Scheil equation and the lever rule (Flemings, 1974; Kurz & Fisher, 1986) to deduce microsegregation from experimental measurements of the temperature of a casting. Macrosegregation was similarly estimated from the Local Solute Redistribution Equation (Flemings & Nereo, 1967). These equations allow the evaluation of various properties of castings given measured values of the evolving temperature field. The prediction of the evolution of a casting

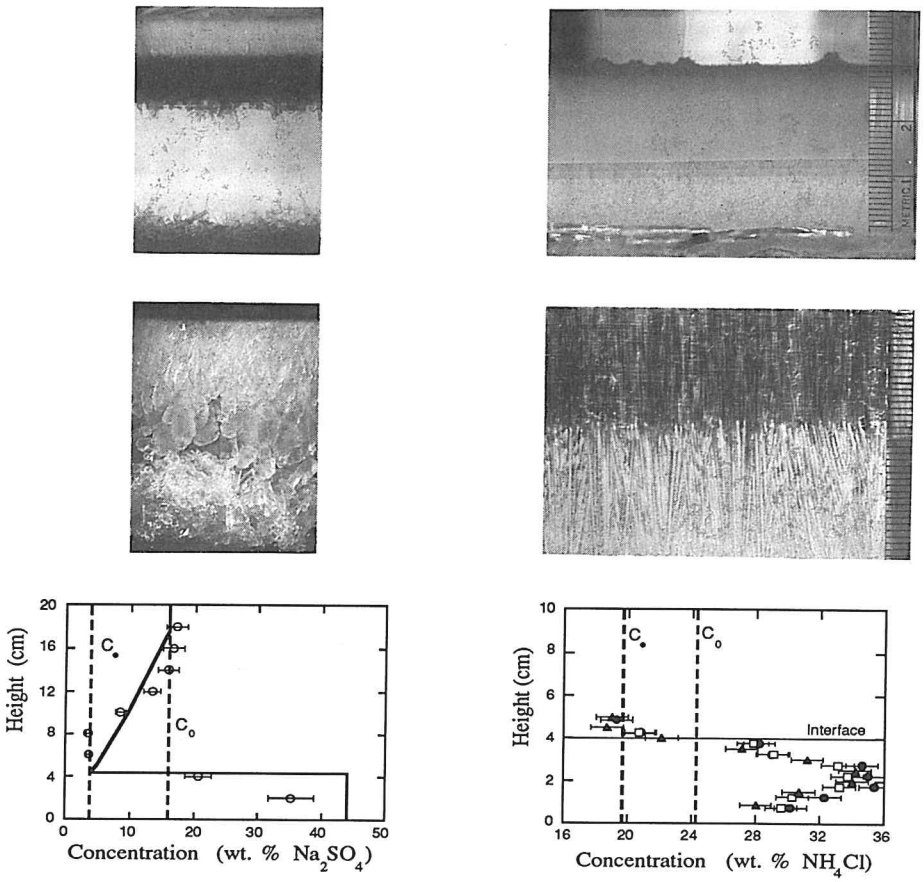

Figure 2. Characteristically different forms of macrosegregation are generated by different types of convection. a) Experiment in which an aqueous solution of sodium sulphate, of initial composition C_0 and eutectic composition C_e, was completely solidified by cooling from above (Kerr *et al.*, 1990c). From the top down, there is a layer of composite, eutectic solid, a mushy layer of sodium-sulphate crystals, a region of melt that is convecting, and a layer of equiaxed crystals on the floor of the tank. b) The final solidified block, showing a distinct change of texture at the columnar-equiaxed transition. c) The symbols show the compositional variation measured in the final solid block. The solid line is the prediction of a mathematical model (Kerr *et al.*, 1990c). d) Experiment in which an aqueous solution of ammonium chloride was completely solidified by cooling from below. A composite eutectic solid layer underlies a mushy layer of ammonium-chloride crystals. The interstitial fluid in the mushy layer is convecting and escapes from the layer through chimneys. e) Close-up of the final solidified block. The structure is all columnar but there is a textural change when ice succeeds ammonium chloride as the primary solidifying phase. f) The compositional variation measured in the final casting. The different symbols correspond to three different corings of the same casting.

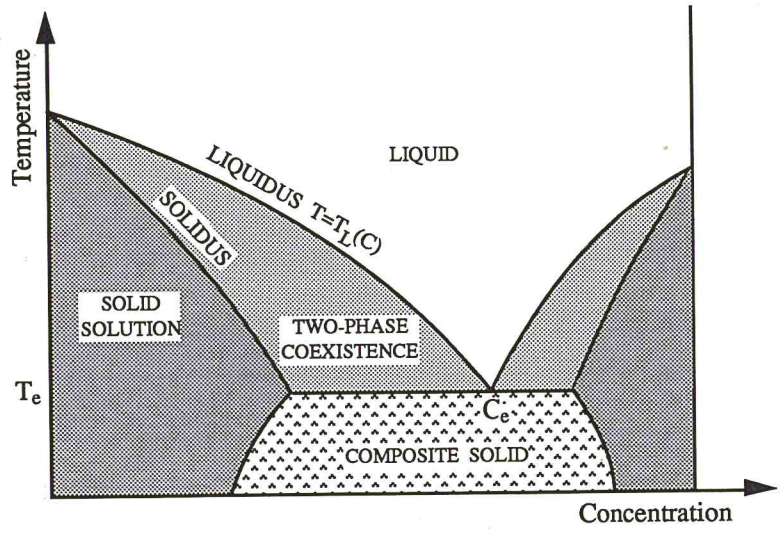

Figure 3. The equilibrium phase diagram of a simple binary alloy. The shaded regions indicate what phases are in thermodynamic equilibrium in a sample of given bulk composition and uniform temperature. If the system remains at equilibrium during cooling then liquid of a particular concentration begins to solidify once the temperature falls below the liquidus curve and is completely solid once the temperature falls below the solidus curve or below the eutectic temperature T_e. When the temperature T and bulk composition are between the liquidus and solidus curves then liquid of the liquidus composition $C_L(T)$ is in equilibrium with solid of the solidus composition given by $kC_L(T)$, which defines the local segregation coefficient $k(C)$.

from the external parameters of the process required additional equations describing fluid flow (Mehrabian *et al.*, 1970) and heat transfer (Fujii *et al.*, 1979). In more recent years, as computers have become more powerful, fully coupled equations describing the transport of mass, heat, momentum and species have been developed and utilized in predictive models of solidifying systems (Szekely & Jassal, 1978; Bennon & Incropera, 1987; Thompson & Szekely, 1988; and see articles by Amberg, Beckermann and Voller in these proceedings, † and references therein). A more philosophical approach was taken by Hills *et al.* (1983) who formulated a very general set of governing equations, based on diffusive mixture theory, that are consistent with fundamental thermodynamical principles. Somewhat different again is the reductionist approach adopted by Huppert & Worster (1985) and Worster (1986), who formulated very simple models that yet contain sufficient information to isolate and explain particular features of the solidification process, and enable quantitative comparisons with laboratory experiments.

† Articles appearing in these proceedings will henceforward be indicated simply by a raised dagger †.

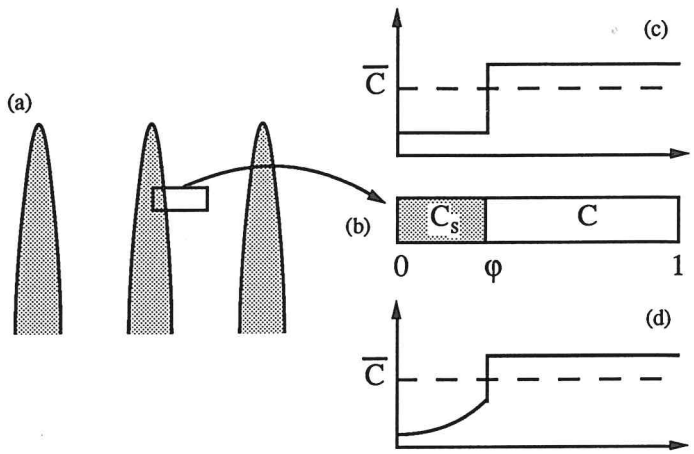

Figure 4. (a) A simplified schematic of a dendritic region. The inset (b) shows the local one-dimensional model used to derive the Scheil equation. (c) The variation of concentration through the solid and liquid regions when there is complete back diffusion. (d) Concentration variation when there is no back diffusion. In each case, the dashed line $\overline{C}$ represents the bulk composition of the element.

2.1 THE SCHEIL EQUATION AND THE LEVER RULE

The mushy layer is a two-phase medium whose properties are determined in large part by the local volume fraction of solid $\phi(\mathbf{x}, t)$, which must be determined as part of the solution of the mathematical model. In most theories to date, the growth or dissolution of solid in the interior of mushy regions is assumed to occur instantaneously, so that the layer is everywhere in local thermodynamic equilibrium. Therefore, the local concentration of the interstitial liquid C and the local temperature T are related to one another through the liquidus

$$T = T_L(C), \tag{2.1}$$

given by the equilibrium phase diagram (figure 3).

The Scheil equation and its close relative, the lever rule, give relationships between ϕ and C. Alternatively, once the equilibrium assumption (2.1) is invoked, these equations can be used to infer the solid fraction once the local temperature is known. These equations can be derived (Kurz & Fisher, 1986) from a local one-dimensional problem (figure 4b) identified from a simplified picture of a dendritic region (figure 4a). The lever rule follows directly from conservation of solute under the assumption of complete local equilibrium in which the solid phase has uniform composition $C_s = kC$, where $k(C)$ is the local value of the segregation coefficient (figure 4c). A simple mass balance, ignoring any change of specific volume on change of phase, gives

$$\phi = \frac{1}{p}\left(1 - \frac{\overline{C}}{C}\right), \qquad \text{where} \qquad p = 1 - k, \tag{2.2}$$

and $\overline{C}$ is the bulk composition of the one-dimensional element (figure 4b).

The lever rule (2.2) is only appropriate if the timescale for diffusion of solute in the solid phase (so-called 'back diffusion') is rapid compared with the timescale for the macroscopic evolution of the mushy region. In fact, a more reasonable approximation in most circumstances is that there is negligible back diffusion, in which case the composition of the solid phase varies across each dendrite; $C_s = C_s(\phi')$, $0 \leq \phi' \leq \phi$. In this case, the composition of the solid phase varies with position, and equilibrium is only imposed at the local solid–liquid interface (figure 4d). Two additional assumptions are made in the derivation of the Scheil equation, namely that the segregation coefficient k is constant, and that the local bulk composition of the element $\overline{C}$ does not change during the evolution of the mushy region. Given these assumptions, it is straightforward to derive the Scheil equation

$$\phi = 1 - \left(\frac{\overline{C}}{C}\right)^{1/p}. \tag{2.3}$$

from conservation of mass of solute.

It has been pointed out (Kurz & Fisher, 1986) that, according to the Scheil equation, $C \to \infty$ as $\phi \to 1$, and that this unphysical singularity is avoided in practice by the process of back diffusion. However, the Scheil equation should rather be interpreted as saying that the solid fraction is bounded away from unity in practical situations, in which the temperature, and hence the local concentration, is always finite, so that the singularity is never encountered.

Neither the lever rule nor the Scheil equation take account of any global redistribution of solute and they give poor approximations whenever flow of the interstitial fluid is significant. The lever rule can be used (provided the assumption of infinite back diffusion is appropriate) if one can determine how the bulk composition is altered by the flow. However, the Scheil equation is never valid once the local bulk composition varies with time. Another way of understanding this is to realise that, if there is no back diffusion or only finite back diffusion, the solid fraction depends not only on the instantaneous value of the bulk composition but on the entire history of its evolution.

2.2 THE MUSHY LAYER AS A CONTINUUM

The need to predict the macroscopic redistribution of solute within the mushy layer requires the development of appropriate transport equations (Flemings & Nereo, 1967; Flemings, 1981; Hills *et al.*, 1983; Worster, 1986; Bennon & Incropera, 1987). Such equations are formulated from fundamental conservation laws applied to 'infinitesimal' control volumes that nevertheless are considered to encompass representative samples of both phases. In this sense, the mushy region is considered as a new continuum phase. Therefore, the resulting description cannot resolve any details on the scale of the spacing between dendrites. Put more positively, the macroscopic predictions of the models that emerge are independent of the structure of the micro scale and can therefore be applied in a wide range of circumstances. For the sake of simplicity, we consider only cases when the solid phase is immobile. The principal assumptions of the model are that, within each infinitesimal control volume, the temperature T is uniform across the solid and liquid phases, the composition of the liquid phase C is uniform and there is no back diffusion of solute within the solid phase.

The properties of the mushy region are local mean properties. For example, the local density is

$$\overline{\rho} = \phi\rho_s + (1-\phi)\rho_l, \tag{2.4}$$

where ρ_s and ρ_l are the densities of the liquid and solid phases, which are assumed to be constant. Mass is only transported by advection of the interstitial fluid, so conservation of mass is expressed by

$$\frac{\partial\overline{\rho}}{\partial t} + \nabla\cdot(\rho_l\mathbf{U}) = 0, \tag{2.5}$$

where $\mathbf{U}$ is the flow rate of the interstitial fluid per unit area. From equation (2.5), it can be determined that the veloctiy field generally has a non-zero divergence given by

$$\nabla\cdot\mathbf{U} = (1-r)\frac{\partial\phi}{\partial t} \tag{2.6}$$

where $r = \rho_s/\rho_l$. Such a velocity can be generated solely in response to the expansion or contraction that occurs due to the difference in density between the liquid and solid phases, and does not require the exertion of any external force such as gravity. The transport caused by this interstitial flow strictly invalidates the Scheil equation and the lever rule, though these often provide adequate approximations in practical situations, especially if the density ratio r is close to unity.

With the approximations stated above, the local mean concentration of solute $\overline{C}$ in the mushy region is given by

$$\overline{\rho}\,\overline{C} = \rho_s\int_0^{\phi} C_s(\phi')\,d\phi' + \rho_l(1-\phi)C. \tag{2.7}$$

Conservation of solute requires that

$$\frac{\partial}{\partial t}\overline{\rho}\,\overline{C} + \nabla\cdot(\rho_l C\mathbf{U}) = \rho_l\nabla\cdot(\overline{D}\nabla C), \tag{2.8}$$

where $\overline{D}$ is the local mean solutal diffusivity of the mushy layer. Equation (2.8) can be expanded and combined with equation (2.6) to give

$$(1-\phi)\frac{\partial C}{\partial t} + \mathbf{U}\cdot\nabla C = \nabla\cdot(\overline{D}\nabla C) + r(1-k)C\frac{\partial\phi}{\partial t}. \tag{2.9}$$

This is a diffusion-advection equation with a source term related to the rate of expulsion of solvent as the local solid fraction ϕ increases.

We shall see later that it is appropriate to neglect the diffusion of solute within the mushy layer provided that the ratio of the solutal diffusivity D to the thermal diffusivity κ is small. With this approximation, and incorporating the equilibrium condition (2.1), equation (2.9) can be written as

$$\frac{\partial\chi}{\partial C} = -\frac{1}{r(1-k)}\left[1 + \frac{\mathbf{U}\cdot\nabla T}{\dfrac{\partial T}{\partial t}}\right]\frac{\chi}{C}, \tag{2.10}$$

where $\chi = 1-\phi$ is the local volume fraction of liquid. This is the Local Solute Redistribution Equation (LSRE), first derived by Flemings & Nereo (1967). They used the equation to determine the macrosegregation in a casting from estimates of the flow field $\mathbf{U}$ and measurements of the temperature field T.

Note that, in the special case of no flow of the interstitial fluid, the LSRE (2.10) can readily be integrated to recover the Scheil equation (2.3).

An equation governing the temperature field in the mushy region is most readily and systematically derived in terms of the local enthalpy $\overline{H}$, where

$$\overline{\rho}\overline{H} = \phi\rho_s H_s + (1-\phi)\rho_l H_l, \tag{2.11}$$

and H_s and H_l are the local enthalpies per unit mass of the solid and liquid phases respectively. In terms of enthalpy, the equation expressing conservation of heat is identical in form to the equation for conservation of solute (2.8) and is given by

$$\frac{\partial}{\partial t}\overline{\rho}\overline{H} + \nabla\cdot(\rho_l H_l \mathbf{U}) = \nabla\cdot(\overline{k}\nabla T), \tag{2.12}$$

where $\overline{k}$ is the mean thermal conductivity of the mushy region. Expanding equation (2.12) using equations (2.6) and (2.11) yields the equation governing the temperature field,

$$\overline{c}\frac{\partial T}{\partial t} + c_l\mathbf{U}\cdot\nabla T = \nabla\cdot(\overline{k}\nabla T) + \rho_s L\frac{\partial\phi}{\partial t}, \tag{2.13}$$

where

$$\overline{c} = \phi c_s + (1-\phi)c_l,$$

and

$$c_{s,l} = \rho_{s,l}\frac{dH_{s,l}}{dT}$$

are the specific heat capacities per unit volume of the solid and liquid phases. The latent heat of solidification per unit mass is defined by $L = H_l - H_s$. Note that in general, L is a function of both temperature and concentration. However, if the phase change always occurs at the equilibrium temperature, given by equation (2.1), then L can be viewed as a function solely of the concentration C of the interstitial liquid.

The three equations (2.6), (2.9) and (2.13) are all coupled through ϕ_t, the rate of change of solid fraction. To complete the model, an evolution equation for ϕ is required. Alternatively, ϕ can be determined implicitly by invoking an assumption of instantaneous reaction, which leads to the application of the equilibrium liquidus relationship (2.1) throughout the mushy region. Thus the temperature T and concentration C are essentially the same variable, mathematically speaking, and the diffusion term in equation (2.9) can safely be neglected, without causing a singular perturbation, when the solutal diffusivity is much smaller than the thermal diffusivity, as is usually the case.

When flow is driven by external agents, such as a gravitational field, or when shrinkage occurs in more than one dimension, a dynamical equation is required for the velocity field in addition to the kinematic equation (2.6). In the fully liquid region, the appropriate equation is the Navier-Stokes equation for viscous fluid flow. In the mushy region, there is

considerable resistance to flow as the fluid passes between the dendrites. It seems appropriate to model the mushy region as a porous medium, the simplest description of which is given by Darcy's equation

$$\mathbf{U} = \Pi\,[(\rho_l - \rho_0)\mathbf{g} - \nabla p]\,, \tag{2.14}$$

where ρ_0 is a reference value of the fluid density, p is the hydrodynamic pressure of the interstitial fluid, and Π is the permeability of the medium. Many investigators, particularly those conducting numerical simulations, have replaced equation (2.14) with hybrids of Darcy's equation and the Navier-Stokes equation (Bennon & Incropera, 1987; Voller *et al.*, 1989; Nandapurkar *et al.*, 1989). This has the advantage of allowing numerical solution of the governing equations on a single computational domain. However, it introduces additional physical parameters to the description of the system that must be estimated before realistic computations can be made.

The transport properties of the mushy region $\overline{D}$, $\overline{k}$, and Π are all functions of the local solid fraction ϕ and of the microscopic morphology of the medium (Beran, 1968). For practical purposes, it has been found that simple volume-fraction weighted averages $\overline{D} = (1-\phi)D_l$ and $\overline{k} = (1-\phi)k_l + \phi k_s$ are adequate to describe the mean solutal diffusivity and thermal conductivity. No experimental determination has yet been made of the appropriate form of the permeability of a mushy region, though a variety of expressions have been used in numerical and analytical calculations and in the interpretation of experimental results. The most common have been the Kozeny-Carmen relationship $\Pi = (1-\phi)^3/\phi$ (Bennon & Incropera, 1987; Chen & Chen, 1991; Tait & Jaupart, 1992) and simple power laws such as $\Pi = (1-\phi)^2$ (Roberts & Loper, 1983; Fowler, 1985) and $\Pi = (1-\phi)^3$ (Worster, 1992).

2.3 INTERFACIAL CONDITIONS

When solving a problem involving solidification, there are prescribed boundary conditions applied at the surfaces of the mould. In addition, there are free internal interfaces between solid and liquid regions or between mushy and liquid regions, for example. The motion of these interfaces is partly determined by conservation laws that can be derived directly from the governing equations for mushy regions. Equations (2.6), (2.9) and (2.13) can be integrated over a small volume spanning the interface, in a frame of reference moving with the normal velocity of the interface V, to yield

$$[\mathbf{n}\cdot\mathbf{U}] = -(1-r)V[\phi], \tag{2.15}$$

$$r(1-k)C[\phi]V = \left[\overline{D}\,\mathbf{n}\cdot\nabla C\right] \tag{2.16}$$

and

$$\rho_s L[\phi]V = \left[\overline{k}\,\mathbf{n}\cdot\nabla T\right], \tag{2.17}$$

where [ ] denotes the change in the enclosed quantity across the interface. Conditions (2.16) and (2.17) are derived under the assumption that the temperature and the composition of the liquid phase are continuous across a mush–liquid interface, and can be used at a solid–liquid interface with C interpreted as the concentration in the liquid region at the interface. However, there may be discontinuities of the solid fraction across the interface.

If the jump in ϕ is prescribed, for example $[\phi] = 1$ across a solid–liquid interface, then conditions (2.15)–(2.17) are sufficient to determine the evolution of the interface, in the

absence of any free energy associated with the curvature of the interface. In the case of an interface between a mushy layer and either a completely solid region or a completely liquid region, another equation is required in order to determine $[\phi]$. Since the governing equations are only first-order for ϕ, only one jump condition can be applied in a given problem. Some authors have imposed continuity of ϕ simultaneously at the mush–liquid interface and at the solid–mush interface, at the expense of one of the conservation laws (2.15)–(2.17). Another common practice is to impose continuity of ϕ at mush–liquid interfaces, though there seems no good reason for doing this *a priori*. An alternative condition, suggested by Worster (1986), is the "marginal equilbrium condition" that the normal temperature derivative at the mush–liquid interface be equal to the normal derivative of the local liquidus temperature,

$$[\mathbf{n}\cdot\nabla T] = [\mathbf{n}\cdot\nabla T_L(C)] \equiv T_L'(C)\,[\mathbf{n}\cdot\nabla C]\,. \tag{2.18}$$

Worster (1986) shows that this condition sometimes leads to $[\phi]$ being non-zero and that in such cases setting $[\phi] = 0$ as the interfacial condition instead of (2.18) renders the governing equations insoluble. However, under most common operating conditions, equation (2.18) coupled with equations (2.16) and (2.17) implies that, in fact, $[\phi] = 0$ at advancing mush–liquid interfaces. Indeed, equation (2.18) shows that the temperature and concentration gradients have equal orders of magnitude in the limit as $D/\kappa \to 0$, where κ is the thermal diffusivity, so the right-hand side of equation (2.16) is negligible in this limit. This same equation thus shows that $[\phi] = 0$ when the diffusivity ratio is small, while equation (2.17) then implies that the temperature gradient is continuous across the interface.

An alternative approach to tracking the interfaces between the phases is to solve the governing equations on a single computational domain. This method, which is used mainly for numerical calculations, obviates the need for interfacial conditions. In such calculations, it is usual for the enthalpy to be used as a dependent variable in place of the temperature and for the position of the interfaces to be found *a posteriori* from calculations of the local solid fraction.

3. Phase-Change Convection (Solidification Shrinkage)

One of the purposes of the mathematical model presented in section 2 is to allow quantitative predictions to be made of macrosegregation within a casting. Such undesirable separation of the constituents of an initially uniform melt during casting is effected by various convective processes within the melt. It is sometimes possible to reduce or even to eliminate convection due to buoyancy forces by cooling from below, provided that the primary solidifying phase leaves behind a dense residual (Huppert & Worster, 1985). Alternatively, the alloy could be cast in a micro-gravitational environment such as inside an orbiting space station. However, none of these contingencies will eliminate the flow of melt due to the expansion or contraction that occurs as a result of the solid and liquid phases having different specific volumes.

It has long been realized that solidification shrinkage is an important mechanism causing macrosegregation in both metallurgical systems (Flemings & Nereo, 1967, 1968) and in geological systems such as magma chambers (Petersen, 1987). In addition there have been quantitative estimates made of the extent of macrosegregation using modifications of the Scheil equation coupled with estimates of the local temperature field during solid-

ification (Flemings & Nereo, 1968; Mehrabian *et al.*, 1970). More accurate calculations can be made by solving the full set of coupled transport equations given in the previous section. In complicated mould geometries, numerical solution of the equations must be sought (Beckermann[†]), but if the mould is cooled from a single planar boundary then one-dimensional, similarity solutions can be found (Vas'kin, 1986; Chiareli & Worster, 1992). These solutions, which serve to illustrate the dependence of the degree of macrosegregation on the external control parameters, will be described briefly here.

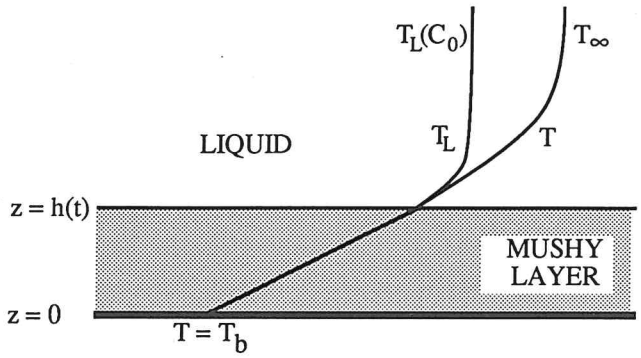

Figure 5. A schematic diagram of a mushy layer growing from a cooled plane boundary when the temperature of the boundary T_b is higher than the eutectic temperature. The temperature T and the local liquidus temperature $T_L(C)$ are illustrated. Far from the cooled boundary, the temperature is T_∞ and the concentration is C_0.

The one-dimensional geometry to be analyzed is illustrated in figure 5. A mushy layer grows in the positive z-direction and has depth $h(t)$ after a time t has elapsed. The boundary $z = 0$ is maintained at the fixed temperature T_b, while the melt far from the interface has temperature T_∞ and concentration C_0. The governing equations and interfacial conditions presented in section 2 admit a similarity solution, in which the dependent variables are functions of the single variable

$$\eta = \frac{z}{2\sqrt{\kappa_l t}}, \tag{3.1}$$

where κ_l is the thermal diffusivity of the liquid phase, and the height of the mush–liquid interface is given by

$$h(t) = 2\lambda\sqrt{\kappa_l t}, \tag{3.2}$$

where λ is a constant to be found as part of the solution. With this transformation of variables, the governing equations reduce to a set of ordinary-differential equations for $T(\eta)$, $C(\eta)$, $\mathbf{U}(\eta)$ and $\phi(\eta)$. In figure 6, the bulk composition $\overline{C}$ at the base of the mushy layer ($\eta = 0$) is plotted as a function of the density ratio $r = \rho_s/\rho_l$. The difference between this bulk composition and the initial concentration of the melt gives a measure of the degree of macrosegregation that has taken place during solidification. It can be seen that the bulk concentration of the casting increases with the density ratio, as shrinkage causes

advection of solute into the mushy layer.

In addition to causing macrosegregation, the flow of interstitial fluid alters the solid fraction of the mushy layer and hence its permeability to flow generated by external forces. Because of the importance of the permeability in determing the strength of convective flow in mushy layers (see section 5) there has been interest recently in measuring the porosity of mushy layers (Chen & Chen, 1991; Shirtcliffe *et al.*, 1991). The latter authors measured the porosity in a system in which ice was solidified from an aqueous solution of sodium nitrate, and compared their measurements with analytical predictions made by Worster (1986). These predictions, in which the expansion during the solidification of ice is ignored, correspond approximately to what would be determined from the Scheil equation. If one takes into account the redistribution of solute caused by expansion then one obtains much better theoretical agreement with the experimental results (figure 7, Chiareli & Worster, 1992). We see from figure 7 that ignoring expansion causes a 10% error in the prediction of the solid fraction. More importantly, the error in the prediction of the porosity (liquid fraction) near the base of the layer is about 50% in this case, which would make a significant difference to the mobility of the interstitial fluid in the presence of external forces.

4. Thermal Convection of the Melt.

Buoyancy forces generated by gradients of temperature and concentration within the melt are the major cause of convection during solidification on Earth. Within the mushy layer, where local equilibrium (equation 2.1) is imposed, the net buoyancy of the interstitial fluid is

$$\Delta\rho = \beta\Delta C - \alpha\Delta T = (\beta - \alpha\Gamma)\,\Delta C, \tag{4.1}$$

where α and β are expansion coefficients for temperature and solute, Γ is the slope of the liquidus curve, and ΔT and ΔC are the temperature and concentration variations across the mushy layer. Under the assumption of local equilibrium, the temperature and solute fields are not free to diffuse independently. Therefore, since $\beta/\Gamma\alpha$ is usually larger than unity, gravitational convection within the mushy layer is determined principally by the solute field.

If a casting is cooled from a horizontal, upper boundary and the primary solidifying phase rejects a less-dense residual then there is no tendency for the interstitial fluid in the mushy layer to convect gravitationally. However, thermal convection of the melt can ensue, since it is being cooled from above. The mushy layer itself can be modelled using the equations of section 2, with r set equal to unity if attention is to be focused on the rôle of thermal convection (Kerr *et al.*, 1990a). The effect of thermal convection in the melt is felt only through the interfacial condition (2.17), in which account must be taken of the convective heat flux from the melt to the mushy layer. Such convection influences the rate of growth of the mushy layer (Turner *et al.*, 1986; Kerr *et al.*, 1990a) but does not by itself cause any macrosegregation of the casting.

However, in laboratory experiments in which aqueous solutions were cooled from above, with all other boundaries of the system insulated, significant macrosegregation of the solidified product has been observed (Turner *et al.*, 1986, Kerr *et al.*, 1990c; figure 2c). The interface between the upper region, where the bulk composition decreases with depth, and the lower region, where the composition increases with depth, was also marked by a

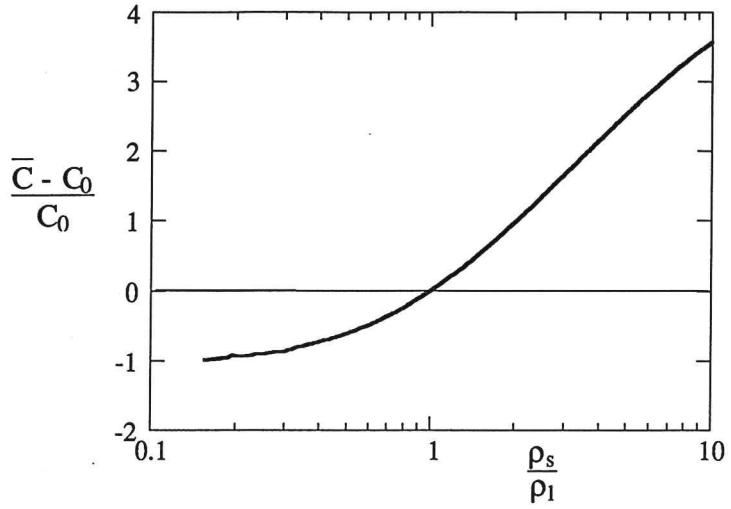

Figure 6. The theoretical macrosegregation caused by solidification shrinkage as a function of the density ratio between solid and liquid. The bulk composition at the base of the mushy layer is $\overline{C}$, while the initial composition of the melt is C_0. The calculations for this graph were made by A.O.P. Chiareli (Ph.D. Northwestern University).

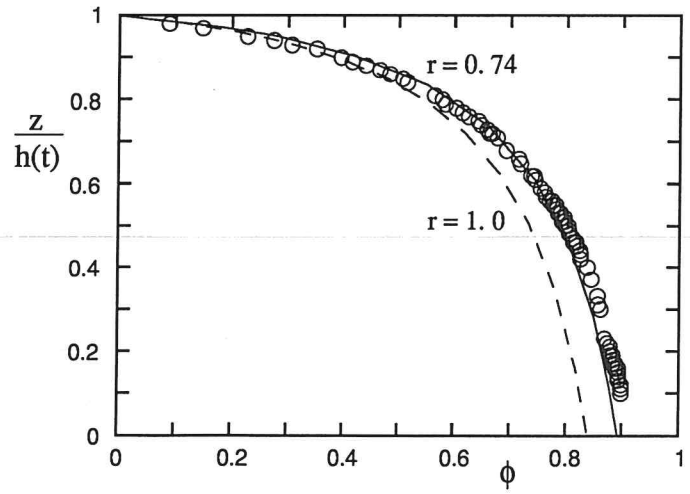

Figure 7. The volume fraction of solid ϕ in a mushy layer as a function of the relative depth in the layer, $z/h(t)$, where $h(t)$ is the height of the layer. The circles are data from experiments of Shirtcliffe *et al.* (1991), using aqueous solutions of sodium nitrate, reinterpreted by Chiareli & Worster (1992). The dashed line is the prediction of a model that negletcts solidification shrinkage ($r \equiv \rho_s/\rho_l = 1$), while the solid line takes full account of the interactions between solidification and the velocity field induced by shrinkage ($r = 0.74$).

so-called "columnar–equiaxed transition". At this interface, vertically-aligned, dendritic crystals attached to the roof of the container met randomly-oriented crystals that had grown in the interior of the melt and had settled and continued to grow at the base of the container.

The columnar-equiaxed transition is very important metallurgically since the different crystal morphologies influence the structural properties of the casting significantly. The growth of equiaxed grains in the interior of the melt (away from the cooled boundaries) cannot be explained by theoretical models that employ all the assumptions of equilibrium thermodynamics since, according to such models, the melt cannot be cooled below its liquidus temperature (Brandeis & Marsh, 1989; Kerr *et al.*, 1990a).

There are two places where equilibrium is imposed in the theoretical model described in section 2: in the interior of the mushy layer; and at the advancing interface between the mushy layer and the liquid region. In reality, there must exist some degree of undercooling (disequilibrium) at all evolving solid–liquid phase boundaries in order to drive solidification, so there must be some disequilibrium associated with the surfaces of individual dendrites within the mushy layer. However, any disequilibrium will also promote morphological instabilities of the dendrite leading to secondary and tertiary side branches. The side-branching activity within the mushy layer will tend to reduce the level of disequilibrium as the consequent increase in specific surface area of micro-scale phase boundaries promotes the release of latent heat and solute into the interstices. Thus the level of disequilibrium can be kept very small in the interior of the mushy layer, and the assumption of local equilibrium there is a good one. Note that the morphological instabilities that lead to side branching are inhibited by the surface energy associated with the curvature of the solid–liquid interface. Therefore, the assumption of internal equilibrium will be less good in systems that have large interfacial energies, especially those systems that display faceted rather than dendritic crystals.

The "interface" between the mushy region and the liquid region does not have a well-defined position on the micro scale. Rather it is a region of some small but finite thickness inhabited by the tips of dendrites. The specific surface area of solid–liquid phase boundaries in this interfacial region may be quite small since significant side-branching only occurs at some distance from the tips of dendrites. Thus the level of disequilibrium may be significant at the mush–liquid interface. It is possible to explain the growth of equiaxed grains in the interior of the melt and the macrosegregation that can additionally occur by relaxing the condition of interfacial equilibrium while maintaining the assumption of internal equilibrium.

A model incorporating a prescribed constant level of undercooling at the interface was proposed by Clyne (1981) and was subsequently extended to include a dynamically variable undercooling by Flood & Hunt (1987). These authors modelled the mushy region using the Scheil equation and an equation equivalent to (2.13) to determine the local temperature. We can describe the way in which disequilibrium was accounted for by these authors, using the terminology of the present paper, as follows. In the limit of zero diffusivity ratio ($D/\kappa \to 0$), the condition of marginal equilibrium at the mush–liquid interface (2.18) implies that the temperature of the interface is given by

$$T_i = T_L(C_\infty), \tag{4.2}$$

where C_∞ is the composition of the liquid far from the interface (strictly, the composition

just outside the compositional boundary layer). Clyne (1981) replaced this condition by

$$T_i = T_L(C_\infty) - T_U, \tag{4.3}$$

where T_U is an assumed-constant value of the interfacial undercooling, while Flood & Hunt (1987) used the condition

$$V = F\left[T_L(C_\infty) - T_i\right]. \tag{4.4}$$

In the kinetic condition (4.4), V is the normal velocity of the interface and $F(\Delta T)$ is some function of the undercooling $\Delta T = T_L(C_\infty) - T_i$. In fact, Flood & Hunt (1987) used the function $F(\Delta T) = \mathcal{G}(\Delta T)^2$, which is appropriate for crystal interfaces growing by screw dislocations (Kirkpatrick, 1975). A similar analysis was carried out by Kerr *et al.* (1990b) using the function $F(\Delta T) = \mathcal{G}\Delta T$, which is more appropriate for molecularly rough crystals. In addition, Kerr *et al.* (1990b) conducted experiments in which a mushy layer of ice crystals was grown from a mixture of water and isopropanol, and were able both to confirm the linearity of the kinetic growth law for that system and to determine the value of the coefficient $\mathcal{G}$.

Although disequilibrium is only imposed locally at the mush–liquid interface, thermal convection of the melt can sweep undercooled liquid from the neighbourhood of the interface into the bulk of the region of melt. Thus the whole melt region becomes supercooled, and any nuclei within the melt can grow to produce large crystals. The heat transfer from these crystals is not directed (as it is in the mushy layer), so the crystals are randomly oriented (equiaxed).

In the model of Flood & Hunt (1987), the equiaxed crystals in the melt were assumed to grow from pre-inserted nucleation sites and remained fixed in space. Therefore, although, the authors were able to draw conclusions regarding the columnar-equiaxed transition, their model did not produce any macrosegregation. By contrast, Kerr *et al.* (1990b) made the assumption that all crystals grown in the interior of the melt settled instantaneously to the bottom of the container to form a uniform layer of solid there. This settling, and the consequent enrichment of the melt of the secondary component causes macrosegregation of the form illustrated in figure 2c. The assumption of instantaneous settling results in an over prediction of the degree of macrosegregation, as does the assumption that the settled crystals form a solid layer rather than a porous pile. As to the cause of macrosegregation in this case; while it is true that there would be none without the settling of crystals or, equivalently, the convection of depleted melt from the neighbourhood of the interior crystals, the root mechanism is the interactive coupling of thermal convection of the melt with the kinetic undercooling of the crystals at the mush–liquid interface.

5. Compositional Convection in the Mushy Region

Buoyancy-driven convection within mushy layers can occur when the composition of the interstitial fluid is unstably stratified. Such is the case for example when an alloy is solidified from below and the primary solidifying phase leaves a less dense residual. Convection of this type was first observed by Copley *et al.* (1970) in experiments in which an aqueous solution of ammonium chloride was solidified from below to form a mushy layer of ammonium-chloride crystals. Similar experiments have since been reported by a number of authors (Roberts & Loper, 1983; Sample & Hellawell, 1984; Chen & Chen, 1991; Tait & Jaupart,

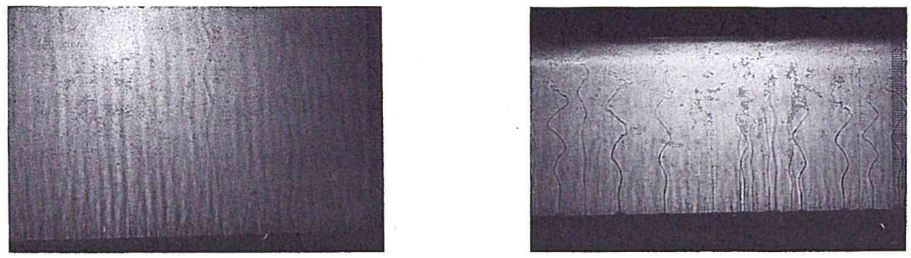

Figure 8. Photographs of the two different types of convection seen in experiments in which solutions of ammonium chloride are cooled and solidified from below. a) Early in the experiment double-diffusive fingers emanate from the vicinity of the mush–liquid interface. b) Later, isolated plumes rise through vents (chimneys) in the mushy layer into the overlying solution.

1992). The evolution of such experiments follows three distinct phases. Initially, a uniform mushy layer grows with a planar interface, and double-diffusive, finger convection rises from the interface a few centimetres into the solution (figure 8a). Once the mushy layer has reached a certain depth, the top of the layer becomes hummocked and chimneys begin to form, through which emanate plumes of buoyant fluid (figure 8b). As the strength of convection through chimneys becomes stronger, the finger convection wanes and eventually disappears. The later stages of the experiments are marked by a gradual decrease in the number of chimneys as the mushy layer deepens.

A full theoretical understanding of these experiments has still not been acheived, though aspects of the observed phenomena have been at least partially explained. One of the principal questions that has intrigued researchers in this field is the mechanism of chimney formation. Perhaps guided by observations of similar structures in fluidized beds (for example in a pot of boiling rice), it was suggested that chimneys might be produced mechanically by convective upflow breaking off the side branches of dendrites (Roberts & Loper, 1983). Hellawell (1987) noticed that he could induce the formation of a chimney by sucking fluid vertically through a pipette near the upper surface of the mushy layer. This observation led to the conjecture that upflow in the double-diffusive fingers above the mushy layer might be the root cause of chimney formation. Mehrabian *et al.* (1970) used the LSRE to deduce the incipiant formation of chimneys in the interior of a mushy region whenever the vertical velocity exceeds the local velocity of the isotherms. The mechanism of formation in this case is the local dissolution of solid (dendrites) within the layer. This idea was echoed by Fowler (1985) who argued additionally that this condition on the velocity field would first be met at the mush–liquid interface and that, therefore, chimneys should be observed growing downwards from the interface into the interior. Dissolution has been shown to be a possible mechanism for chimney formation in large-scale numerical

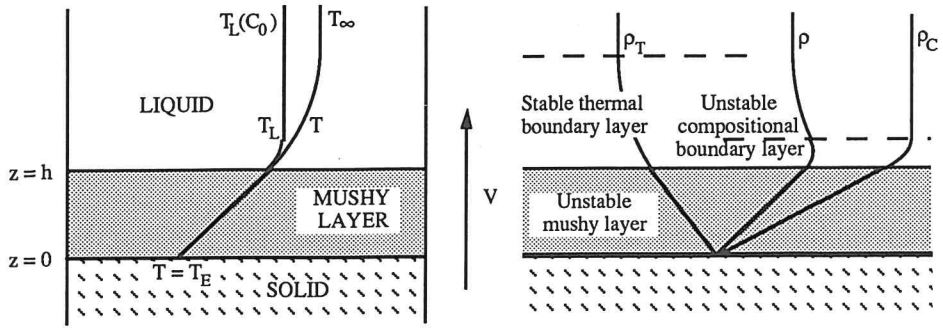

Figure 9. a) A schematic diagram of a binary melt being solidified at a constant rate from below. The temperature is fixed at the eutectic temperature at the horizontal position $z = 0$ in a frame moving with the constant solidification speed V. The temperature field T and the local liquidus temperature $T_L(C)$ are illustrated. b) The density distributions caused by the temperature field ρ_T, the solute field ρ_C and the total density of the liquid ρ. The density field in the mushy layer is statically unstable in a gravitational field directed vertically downwards, as is the density in the compositional boundary layer just above the mush–liquid interface.

calculations by Bennon & Incropera (1988) and in a linear-stability analysis by Worster (1992). All this does not rule out the possibility of a substantial rôle being played by mechanical shearing of side branches, however. Recent work by Glicksman† shows how local dissolution and ripening effects cause a necking of the side branches, possibly to a point where they can be easily torn off by a weak flow. In addition, observations by Sarazin & Hellawell† clearly show crystal fragments being carried upwards out of chimneys by the convecting plumes.

5.1 STABILITY THEORY

The prediction of when, rather than how, chimneys form can begin to be answered by an analysis of the stability of a mushy layer to the onset of buoyancy-driven convection. The governing equations presented in section 2 have a steady solution in a frame of reference moving with a prescribed vertical speed V, (see figure 9a). In the absence of any flow, the steady temperature and concentration fields give rise to the density field illustrated in figure 9b. The mushy layer is unstably stratified and, in addition, there is a narrow unstable boundary layer just above the mush–liquid interface.

The first analysis of the convective stability of a mushy layer was conducted by Fowler (1985), who analyzed a special limit of the governing equations, in which the compositional boundary layer has negligible thickness and the solid fraction in the mushy layer is zero. The stability problem reduces to that of the stability of a fixed porous medium with a solid lower boundary and a condition of zero pressure applied to the upper boundary. Chen & Chen (1988) presented an analysis of the stability of a fluid layer above a fixed porous medium, with a uniform, unstable temperature gradient applied across them. This arrangement mimics the compositional boundary layer above the mushy layer illustrated in figure 9b. They found a bi-modal marginal-stability curve similar in form to that shown

in figure 10. A stability analysis using the full transport equations for the mushy layer was conducted by Nandapurkar *et al.* (1989). However, they did not allow perturbations of the solid fraction, and thereby suppressed any interaction between the convective flow and the growth of solid. They considered a single set of physical parameters and found just one mode of convection that did not penetrate the mushy layer.

Fully coupled interactions between flow and solidification were also considered in a normal-mode analysis by Worster (1992). He found that, in general, the marginal-stability curve is bimodal (figure 10), with the structure of the flow in the two modes as shown in figure 11. One mode, the "mushy-layer mode", has a horizontal wavelength comparable to the depth of the mushy layer, while the other, the "boundary-layer mode" has a wavelength comparable to the thickness of the compositional boundary layer above the mush–liquid interface. In effect, Fowler (1985) had analyzed a special case of the mushy-layer mode, while Nandapurkar *et al.* (1989) had found the boundary-layer mode. Either mode can be the more unstable depending on the parameters of the system (Worster, 1992), though for the parameter values of a typical laboratory experiment, the boundary-layer mode is found to be unstable long before the mushy-layer mode.

Since the flow in the boundary-layer mode does not penetrate the mushy layer, this mode has little influence on the solid fraction within the layer. By contrast, the mushy-layer mode causes the perturbations to solid fraction shown in figure 12. The interface is elevated in regions of upflow and the solid fraction through most of the depth of the layer is decreased there. These features are consistent with the form of chimneys observed in laboratory experiments, and suggest that it is the mushy-layer mode of convection that is primarily responsible for the formation of chimneys.

The sequence of events in a typical laboratory experiment might be explained as follows. Very soon after the start of an experiment, the boundary-layer mode becomes unstable and gives rise to double-diffusive plumes above the mushy layer. Sometime later, when the mushy layer is deeper, the Rayleigh number associated with the layer exceeds the critical value for the mushy-layer mode, and convection throughout the layer is initiated. This convection causes the interface to be elevated in regions of upflow, and depressed elsewhere, which gives rise to the hummocky appearance of the mushy layer. If the mushy-layer mode is sub-critically unstable then large perturbations, such as sucking, might trigger the early onset of the mode, which would explain the observations of Hellawell (1987).

If it is true that the mushy-layer mode gives rise to chimneys then it is of some importance to determine the conditions under which it is unstable. The Rayleigh number determining the convective stabilty of the mushy layer is

$$R_m = \frac{\beta \Delta C g \Pi^* H}{\kappa \nu}, \tag{5.1}$$

where g is the acceleration due to gravity, ν is the kinematic viscosity of the fluid, H is a length scale, such as the unperturbed depth of the mushy layer, and Π^* is a representative value of the permeability of the layer. Quantitative prediction of the onset of convection in a physical situation is complicated by the difficulty of determining the permeability of a mushy layer. Tait & Jaupart (1992) made estimates of the permeability in their experiments with ammonium chloride by measuring the mean separation of primary dendrite arms and applying an equation derived for the permeability of a vertical array of cylinders. This allowed them to estimate the critical Rayleigh number from observations of when the mushy layer first appeared hummocky. Some of their results are reproduced in figure 13,

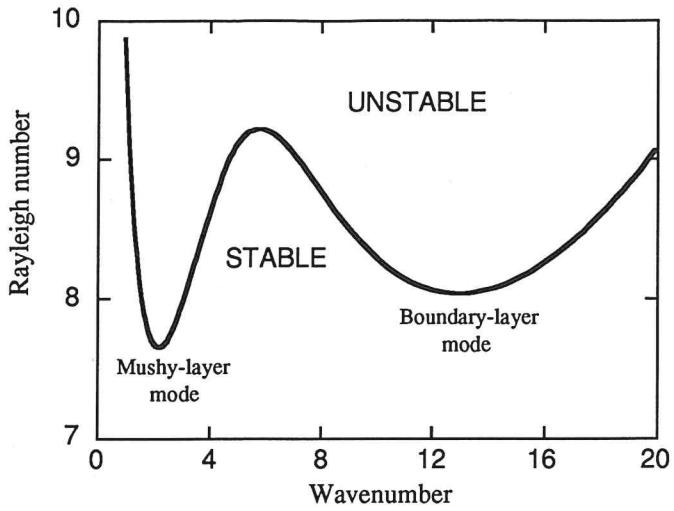

Figure 10. The marginal-stability curve for the onset of compositional convection in the system illustrated in figure 9. The two minima correspond to distinct modes of convection, as illustrated below. This graph was calculated for the diffusivity ratio $D/\kappa = 0.025$ and the ratio $H^2/\Pi^* = 10^5$, where $H = \kappa/V$ is the length scale for thermal diffusion and Π^* is a reference value of the permeability of the mushy layer. Either mode can be the more unstable depending on the values of these parameters (Worster, 1992).

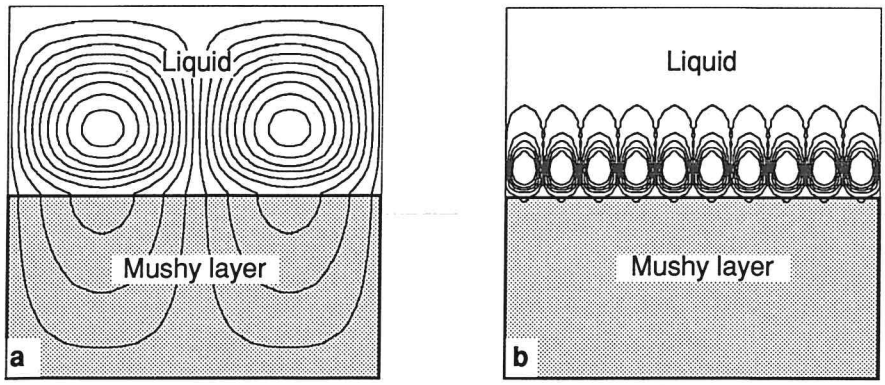

Figure 11. Streamlines for the marginally-stable modes corresponding to the two minima in figure 10. a) The mushy-layer mode has a wavelength comparable to the depth of the mushy layer and the flow penetrates the layer. b) The boundary-layer mode has a wavelength comparable to the thickness of the compositional boundary layer above the mush-liquid interface. The flow in this mode barely influences the underlying mushy layer.

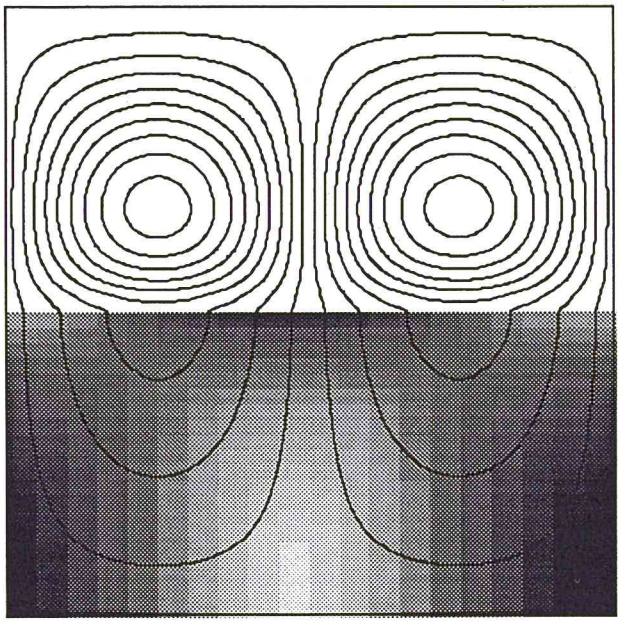

Figure 12. The perturbations to the solid fraction caused by the mushy-layer mode of convective instability. Dark regions show where the solid fraction has increased while lighter regions indicate where the crystals have dissolved. In regions of upflow, the solid fraction is generally decreased while the mush–liquid interface is elevated (indicated by the dark patch near the top of the mushy layer).

where they are compared with the predictions of the linear-stability analysis of Worster (1992). There is some scatter in the data but the general trend that the critical Rayleigh number decreases as the far-field temperature increases is found both in the theory and the experiments.

5.2 FULLY-DEVELOPED CHIMNEYS

As important as knowing when chimneys will occur is to know what their effect is once their occurence is unavoidable. For example, the convective flow through chimneys causes an exchange of solute between the mushy layer and the overlying region of melt that results in macrosegregation of the casting (figure 2f). In order to make predictions of the extent of macrosegregation it is necessary to be able to calculate the flux of solute through the chimneys. The flow through the mushy layer feeding the upflow through chimneys was first addressed by Roberts & Loper (1983). They showed that the flow through each chimney is similar to that through a thermosyphon (Lighthill, 1953) and calculated the flow through the surrounding mushy layer, whose solid fraction was taken as a fixed function of depth. These calculations were extended by Worster (1991), who analyzed the flow in the asymptotic limit of large Rayleigh number. He found that, in this limit, there is a

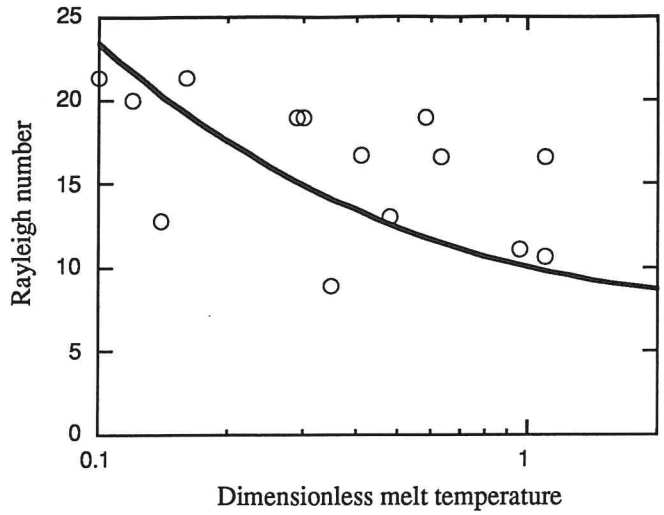

Figure 13. The critical Rayleigh number as a function of the far-field temperature of the melt given parameter values appropriate for an aqueous solution of ammonium chloride. The solid line shows the prediction of a stability analysis. The data are from experiments by Tait & Jaupart (1992).

thermal boundary layer around each chimney, in which the solid fraction is larger than in the rest of the mushy layer as a result of additional cooling by the fluid rising through the chimney. This increased crystal growth can be seen in experiments, and is the likely cause of the 'volcanic vent' around the top of each chimney (figure 8b). The asymptotic analysis allows calculation of the fluxes of mass, heat and solute through each chimney. The overall strength of the convective exchange between the mushy layer and the overlying liquid depends, in addition, on the areal number density of chimneys.

From his asymptotic analysis, Worster (1991) determined a family of solutions for the temperature, composition and solid fraction in the mushy layer, parameterized by the number density of chimneys. The fluxes of heat F_T and solute F_C from the mushy layer to the overlying fluid are given by

$$F_T = -\rho C_p \mathcal{F} V (T_\infty - T_L(C_0)) \tag{5.2}$$

and

$$F_C = -\tfrac{1}{2}\mathcal{F} V (C_0 - C_b), \tag{5.3}$$

where T_∞ and C_0 are the temperature and composition of the melt, C_b is the composition of the interstitial fluid at the base of the mushy layer, V is the rate of solidification, and $\mathcal{F}$ is a parameter proportional to the number density of chimneys. These expressions can be used to determine a relationship between the temperature and the composition of the liquid region

$$T = T_L(C_0) + (T_\infty - T_L(C_0)) \left[1 - \frac{C - C_0}{C_0 - C_b}\right]^2 - (T_L(C_0) - T_b) \left(\frac{C - C_0}{C_0 - C_b}\right)^2. \tag{5.4}$$

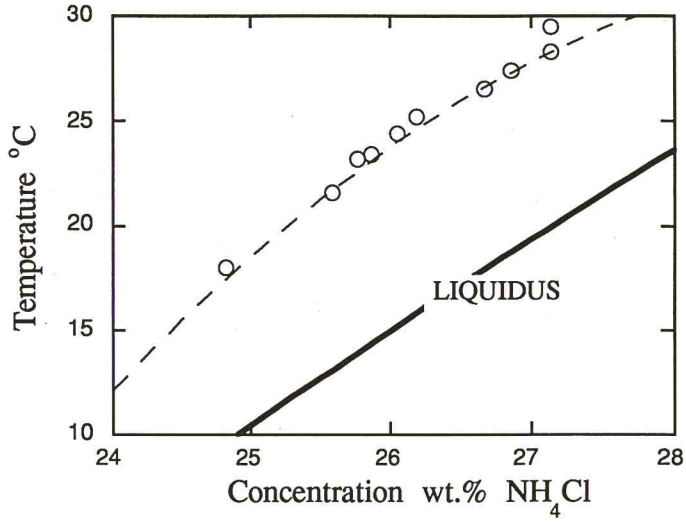

Figure 14. The evolution of the temperature and composition of the melt above a mushy layer caused by convection through chimneys in the layer. The data are from an experiment using an aqueous solution of ammoinium chloride. The dashed line is the predition of an asymptotic analysis in the limit of large Rayleigh number (Worster, 1990, 1991).

This expression is plotted in figure 14, where it is compared with measurements from an experiment using an aqueous solution of ammonium chloride. There is good agreement between the theoretical results and the experimental measurements, but the result is of limited use. In order to make individual predictions of the evolution of the temperature and solute fields, and hence the rate of solidification and the extent of macrosegregation, it is necessary to find some way to predict the number density of chimneys, or alternatively to determine the parameter $\mathcal{F}$ directly.

However, expression (5.4) and figure 14 do serve to illustrate a particular feature of chimney convection, namely that the temperature of the melt remains above the liquidus temperature. Huppert (1990) pointed out that this behaviour is distinct from what is found in experiments using some other aqueous solutions, in which the melt became supercooled. In these experiments, convection is only seen emanating from the vicinity of the mush–liquid interface, so it might be associated with the boundary-layer mode. As discussed in section 4, significant disequilibrium (undercooling) can exist at the mush-liquid interface, which could be carried into the interior of the melt by the boundary-layer mode of convection. By contrast, when chimneys are present, the flow is primarily downwards into the mushy layer, where the fluid can be restored to near-equilibrium conditions before being ejected through chimneys. During ascent through a chimney, the fluid reaches thermal equilibrium with its surroundings but its composition remains unchanged. It therefore emerges from the chimney undersaturated (superheated). Whether the melt becomes supercooled or not will have a profound influence on the form of macrosegregation and the possibility of columnar-equiaxed transitions.

6. Future Directions

In this review, I have tried to highlight with a few specific examples key interactions that can occur between soldification in mushy layers and the flow of the melt. It is apparent that significant advances have been made in our understanding of mushy layers through a combination of mathematical models and quantitative laboratory experiments. In particular, it now seems certain, from the excellent agreement obtainable between theoretical predictions and experimental data, that mushy layers in which the interstitial fluid is stagnant, or which only moves in response to shrinkage, are well characterized and quantified by the continuum theories. However, while many qualitative aspects of buoyancy-driven convection through the interstices of mushy layers are understood, considerable work still needs to be done before accurate quantitative predictions can be made.

Perhaps the most important subject that needs to be addressed is the appropriate form of the momentum equation in mushy layers and the determination of the associated transport parameters. Even in the simplest cases when Darcy's equation is appropriate, there is a need to determine how the permeability varies as the mushy layer evolves. In general, the permeability Π of a porous medium depends on its porosity χ (liquid fraction) and on the specific surface area M of its internal, wetted surfaces (phase boundaries).

Experimental determinations of the porosity of mushy layers are already being undertaken (Chen & Chen, 1991; Shirtcliffe *et al.*, 1991) and the experimental techniques for doing so will undoubtedly improve in the next few years. Measuring the specific surface area of internal phase boundaries will pose greater difficulties but may not be beyond modern computerized imaging techniques, for example. Even once these two properties of the medium are determined, obtaining the permeability is not straightforward. Many different relationships for the permeability in terms of the porosity and the specific surface area have been proposed, a popular choice being the Kozeny equation (Bear, 1988) which gives $\Pi = c_0\chi^3/M^2$, where c_0 is a constant.

From a theoretical point of view, the variation of porosity has already been taken into account in theories of mushy layers but little attention has yet been given to the evolution of the specific surface area of internal phase boundaries. There are at least two competing influences on the surface area: morphological instabilities that lead to side branches; and surface-energy effects that lead to coarsening. The instabilities of individual, isolated dendrites have been addressed in the past (Langer, 1980) though one suspects that the characteristics of these instabilities will be changed considerably once the dendrite forms part of an array within a mushy region. There have also been experimental (Marsh & Glicksman, 1987) and theoretical (Voorhees, 1985) studies of coarsening in single-component systems. The theoretical studies have a statistical nature that is suitable for application to mushy layers but there is a need to extend them to binary systems and to systems that are evolving due to imposed macroscopic temperature gradients.

Evolution of the internal phase boundaries will only take place in the presence of microscale gradients of temperature and/or solute concentration. This signals the need to relax two of the principal assumptions upon which current theories of mushy layers are based, namely the uniformity of the interstities and local equilibrium of the mushy region. We have already seen that local disequilibrium at a mush–liquid interface, coupled with convection,

has important consequences for macrosegregation of a casting. Depending on the geometry of the casting and the nature of the crystals, flow of the melt will penetrate different depths of a mushy region and it is therefore important to know the extent of significant disequilibrium. Loper† has formulated a non-equilibrium theory of a mushy region which might form the basis for future investigations.

Disequilibrium is also a significant issue in the study of melting within mushy regions, which has yet received little attention. Some aspects of the melting of binary solids have been analyzed by Woods (1992), and the melting of side braches of dendrites has been investigated experimentally by Glicksman†. Localized melting of the solid phase within mushy regions is important for the formation of chimneys, for example, and similar phenomena occur during the slow percolation of groundwater thorugh porous rocks (Phillips, 1991). Whereas morphological instabilities act to keep the specific surface area of internal phase boundaries large during solidification, no such effect occurs during melting, so the micro-scale gradients of temperature and solute concentration that cause internal disequilibrium can be sustained.

One of the major strengths of the theoretical models of mushy regions that have been developed and utilized during the past several years is their independence of the morphology of internal phase boundaries. This has rendered them universally applicable regardless of the chemical species being solidified. To address the challenges of the future (disequilibrium, permeability to fluid flow, coarsening and melting) much more specific information about the chemical system will be required. In addition, there will be an increasing need to include micro-scale phenomena into models of macro-scale processes. Interactions between scientists from the various disciplines dealing with solidification and transport processes will be greatly advantageous in this endeavour.

Acknowledgements

I am grateful to S.H. Davis and H.E. Huppert for their helpful review of early drafts of this review. My research is partially supported by the Thermal Systems Program of the National Science Foundation.

References

Bear, J. (1988) *Dynamics of Fluids in Porous Media.* Dover.

Bennon, W.D. & Incropera, F.P. (1987) A continuum model for momentum, heat and species transport in binary solid–liquid phase change systems — I. model formulation. *Int. J. Heat Mass Transfer* **30**, 2161–2170.

Bennon, W.D. & Incropera, F.P. (1988) Numerical analysis of binary solid-liquid phase change ... a continuum model. *Numerical Heat Transfer* **13**, 277–...

Beran, M.J. (1968) *Statistical Continuum Theories.* Interscience Publishers, New York.

Brandeis, G. & Marsh, B.D. (1989) The convective liquidus in a solidifying magma chamber: a fluid dynamic investigation. *Nature* **339**, 613–616.

Chen, F. & Chen, C.F. (1988) Onset of finger convection in a horizontal porous layer underlying a fluid layer. *Trans. ASMEC: J. Heat Transfer* **110** 403–407.

Chen, F. & Chen, C.F. (1991) Experimental study of directional solidification of aqueous ammonium chloride solution. *J. Fluid Mech.* **227** 567–586.

Chiareli, A.O.P. & Worster, M.G. (1992) On the measurement and prediction of the solid fraction within mushy layers. (preprint, Northwestern University)

Clyne, T.W. (1981) In:Proc. 2nd Intern. Conf. on Numerical Methods in Thermal Problems, Venice, Italy 240–256.

Copley, S.M., Giamei, A.F., Johnson, S.M. & Hornbecker, M.F. (1970) The origin of freckles in binary alloys. *IMA J. Appl. Maths* **35**, 159–174.

Flemings, M.C. (1974) *Solidification Processing.* Mc.Graw Hill.

Flemings, M.C. (1981) in *Modeling of Casting and Welding Processes* (eds. Brody, H.D. & Arpelian, D.), pp. 533–548. The Metallurgical Society of the American Institute of Mining, Metallurgical and Petroleum Engineers, Warrendale.

Flemings, M.C. & Nereo, G.E. (1967) Macrosegregation, part I. *Trans. Met. Soc. AIME* **239**, 1449–1461.

Flemings, M.C. & Nereo, G.E. (1968) Macrosegregation, part III. *Trans. Met. Soc. AIME* **242**, 50–55.

Flood, S.C. & Hunt, J.D. (1987) A model of a casting. *Appl. Sci. Res.* **44**, 27–42.

Fowler, A.C. (1985) The formation of freckles in binary alloys. *IMA J. Appl. Maths* **35**, 159–174.

Fowler, A.C. (1987) Theories of mushy zones: applications to alloy solidification, magma transport, frost heave and igneous intrusions. In *Structure and Dynamics of Partially Solidified Systems* (ed. D.E. Loper), pp. 161–199. NATO ASI Series. Martinus Nijhoff.

Fujii, T., Poirier, D.R. & Flemings, M.C. (1979) *Metall. Trans. B* **10B**, 331–339

Hellawell, A. (1987) Local convective flows in partially solidified alloys. In *Structure and Dynamics of Partially Solidified Systems* (ed. D.E. Loper), pp. 3–22. NATO ASI Series. Martinus Nijhoff.

Hills, R.N., Loper, D.E. & Roberts, P.H. (1983) A thermodynamically consistent model of a mushy zone. *Q. J. Mech. Appl. Maths* **36**, 505–539.

Huppert, H.E. (1990) The fluid dynamics of solidification. *J. Fluid Mech.* **212**, 209–240.

Huppert, H.E. & Worster, M.G. (1985) Dynamic solidification of a binary melt. *Nature* **314**, 703–707.

Kerr, R.C., Woods, A.W., Worster, M.G. & Huppert, H.E. (1990a) Solidification of an alloy cooled from above. Part 1. Equilibrium growth. *J. Fluid Mech.* **21**[illegible]–342.

Kerr, R.C., Woods, A.W., Worster, M.G. & Huppert, H.E. (19[illegible]0b) Solidification of an alloy cooled from above. Part 2. Non-equilibrium interfacial kinetics. *J. Fluid Mech.* **217** 331–348.

Kerr, R.C., Woods, A.W., Worster, M.G. & Huppert, H.E. (1990c) Solidification of an alloy cooled from above. Part 3. Compositional stratification within the solid. *J. Fluid Mech.* **218** 337–354.

[illegible]patrick, R.J. (1975) Crystal growth f[illegible]he melt: a review. *American Mineralogist* **60**, 798–[illegible]

[illegible]. & Fisher, D.J. (1986[illegible]*s of Solidification.* Tans. Tech. Publications.

Lig[illegible]hill, M.J. (1953) T[illegible]ical considerations on free convection in tubes. *Quart. J. Mech. Appl. Math.* **6**, 3[illegible]

Langer, J.S. (1980) Instabilities and pattern formation in crystal growth. *Rev. Mod. Phys.* **52**, 1–28.

Marsh, S.P. & Glicksman, M.E. (1987) Evolution of lengthscales in partially solidified systems. In *Structure and Dynamics of Partially Solidified Systems* (ed. D.E. Loper), pp. 25–35. NATO ASI Series. Martinus Nijhoff.

Mehrabian, R., Keane, M. & Flemings, M.C. (1970) Interdendritic fluid flow and macrosegregation: influence of gravity. *Metall. Trans.* **1**, 1209–1220.

Mullins, W.W. & Sekerka, R.F. (1964) Stability of a planar interface during solidification of a dilute binary alloy. *J. Appl. Phys.* **35**, 444–451.

Nandapurkar, P., Poirier, D.R., Heinrich, J.C. & Felicelli, S. (1989) Thermosolutal convection during dendritic solidification of alloys: Part 1. Linear stability analysis. *Metallurgical Transactions B* **20B**, 711–721.

Petersen, J.S. (1987) Crystallization shrinkage in the region of partial solidification: implications for silicate melts. In *Structure and Dynamics of Partially Solidified Systems* (ed. D.E. Loper), pp. 417–435. NATO ASI Series. Martinus Nijhoff.

Phillips, O.M. (1991) *Flow and Reactions in Permeable Rocks.* Cambridge University Press.

Roberts, P.H. & Loper, D.E. (1983) Towards a theory of the structure and evolution of a dendrite layer. *Stellar and Planetary Magnetism*, 329–349.

Sample, A.K. & Hellawell, A. (1984) The mechanisms of formation and prevention of channel segregation during alloy solidification. *Metallurgical Transactions A* **15A**, 2163–2173.

Shirtcliffe, T.G.L., Huppert, H.E. & Worster, M.G. (1991) Measurement of solid fraction in the crystallization of a binary melt. *J. Crystal Growth* **113**, 566–574.

Szekely, J. & Jassal, A.S. (1978) An experimental and analytical study of the solidification of a binary dendritic system. *Metall. Trans. B* **9B**, 389–398.

Tait, S. & Jaupart, C. (1992) Compositional convection in a reactive crystalline mush and the evolution of porosity. *J. Geophys. Res.* (in press).

Turner, J.S., Huppert, H.E. & Sparks, R.S.J. (1986) Komatiites II: Experimental and theoretical investigations of post-emplacement cooling and crystallization. *J. Petrol.* **27**, 397–437.

Thompson, M.E. & Szekely, J. (1988) Mathematical and physical modelling of double-diffusive convection in aqueous solutions crystallizing at a vertical wall. *J. Fluid Mech.* **187**, 409–433.

Vas'kin, V.V. (1986) Solving solidification equations for a binary alloy by similarity. *Izvestiya Akademii Nauk SSSR, Metally* **1** 83–87. Published by Allerton Press.

Voller, V.R., Brent, A.D. & Prakash, C. (1989) The modelling of heat, mass and solute transport in solidification systems. *Int. J. Heat Mass Transfer* **32**, 1719–1731.

Voorhees, P.W. (1985) The theory of Ostwald ripening. *J. Stat. Phys.* **38**, 231–252.

Woods, A.W. (1992) Melting and dissolving. *J. Fluid Mech.* **239**

Worster, M.G. (1986) Solidification of an alloy from a cooled boundary. *J. Fluid Mech.* **167**, 481–501.

Worster, M.G. (1990) Structure of a convecting mushy layer. *Appl. Mech. Rev* **43, 5** S59–S62.

Worster, M.G. (1991) Natural convection in a mushy layer. *J. Fluid Mech.* **224**, 335–359.

Worster, M.G. (1992) Instabilities of the liquid and mushy regions during solidification of alloys. *J. Fluid Mech.* **237**, 649–669.